

Locating Damage Source in High Pressure CFRP Gas Tank for Space Rocket using AE Measurement

FUKUMOTO Shintaro : Technical Research & Development Center, IHI Inspection & Instrumentation Co., Ltd.

NISHIDO Takayuki : Doctor of Engineering, General Director, Technical Research & Development Center, IHI Inspection & Instrumentation Co., Ltd.

ARAKAWA Takahiro : Doctor of Engineering, Fellow, IHI Inspection & Instrumentation Co., Ltd.

OMORI Mami : Inspection Technology Department, Inspection Division, IHI Inspection & Instrumentation Co., Ltd.

OMORI Seichi : Production Technology Department, Production Engineering Center, Corporate Research and Development

We have been studying damage evaluation methods during the hydraulic test of the thin-walled CFRP pressure vessel using three-dimensional source location (3D source location). In this study, we conducted 3D source location using water propagation waves when the CFRP pressure vessel was damaged. Also, we evaluated the separation tendency of surface propagation waves and water propagation waves, thereby confirming the Kaiser effect. In order to improve the precision of 3D source location using water propagating waves, we demonstrated a new method, "Area locating." The results thereof confirmed that 3D source location using "Area locating" was consistent with fracture phenomenon. In addition, the new method was able to identify the origin of the fracture.

1. Introduction

There are many examples of applying a Carbon Fiber Reinforced Plastic (CFRP) material to space products. Among the space products, there is a pressure tank which is designed to store high-pressure gas in order to push the fuel out from a fuel tank of a satellite propulsion system.

The tank may be damaged during manufacturing and/or transportation. In addition, the damaged tank may be repaired. In such a case, a useful method to check the soundness of a damaged part and/or a repaired part is Acoustic Emission (AE) measurement. In particular, the soundness of a CFRP tank is checked by a pressure proof test after manufacturing and a subsequent non-destructive inspection. The AE measurement in the pressure proof test can specify which part of the tank is damaged at which stage of the test. Therefore, we have to establish a technology enabling the application of the AE measurement during the pressure proof test.

2. Source location of tank by AE method

The AE test is widely spread as a method for evaluating the soundness of a pressure vessel, and standards such as an American Society of Mechanical Engineers (ASME) standard are also established⁽¹⁾⁻⁽³⁾. In the AE test, AE parameter analysis can locate the occurrence of AE, which is called source location. In the AE parameter analysis, for each event, AE waves sensed by multiple AE sensors attached to a test object are classified, and arrival time differences among classified AE waves sensed by the respective AE sensors

serve as AE parameters. In general, AE-based source location is performed using waves propagating on the surface of an object (surface propagation wave)⁽⁴⁾⁻⁽⁶⁾. However, the CFRP material has acoustic anisotropy, and applying a general source location method thereto is difficult.

In the past, using an artificially emitted AE wave, we have confirmed that during a water pressure proof test of a thin-walled CFRP tank, the AE wave well propagates under water. Also, we have shown a new finding on three-dimensional source location by sensing the wave propagating under water by multiple AE sensors⁽⁷⁾.

In this study, we fabricated a CFRP tank having a carbon fiber winding thickness of 6 mm and similar in structure to the above described CFRP thin-walled tank, and performed a water pressure proof test on it. In addition, we used not an artificially emitted AE wave but AE waves generated when damage was developed by raising pressure. For three-dimensional source location using underwater propagation waves, the results of the pressure proof test of the tank after artificially damaged were used. In addition, we aimed to improve the accuracy of the source location.

3. Outline of test

3.1 Specifications of CFRP tank

Figure 1 illustrates the thin-walled CFRP tank, in which the appearance and enlarged surface are respectively illustrated in **Figs. 1-(a)** and **-(b)**. The specifications of the tank are listed as follows. Note that the proof pressure refers to a pressure value up to which a manufacturer of the tank guarantees the soundness of the vessel, but not to a pressure



Fig. 1 Thin-walled CFRP pressure vessel

value at which the vessel is fractured.

Carbon fiber winding thickness	6 mm
Dimensions	
Outside diameter	260 mm
Inside diameter	218 ± 2 mm
Total length	1 150 mm
Liner resin material	Polyethylene resin
Metal cap material	Aluminum 6061-T6 (JIS H 0001)
Proof pressure	7 to 8 MPa
Manufacturing conditions	
Helical hoop winding finishing of T700-compatible carbon fiber by a Filament Winder (FW) process → Full wrap winding processing on resin liner → thermal cure processing → After manufacturing, pressurization to proof pressure	

Note that T700 is the trade name of carbon fiber manufactured by A company, and the denier of it representing the thickness of a fiber or a yarn is 800 g/1 000 m.

3.2 Test system

The specifications of a test system and sensors used are as follows.

AE system	AMSY-6 MB-19 (by Vallen, Germany)
AE emission source	VS150-RIC (by Vallen, Germany)
AE sensors	Frequency band 100 to 500 kHz AE144A (by Vallen, Germany)
Preamplifiers	34 dB, AEP5 (by Vallen, Germany)

3.3 Sensor arrangement and artificial flaw

Figure 2 illustrates the arrangement of sensors attached to the tank and a point of an artificial flaw. In this test, 12 sensors were used. Also, Figure 3 illustrates the artificial flaw formed by a grinder, in which the situation when the artificial flaw was provided is illustrated in Figure 3-(b).

3.4 Water pressure proof test

Figure 4 illustrates steps of the water pressure proof test. In the water pressure proof test No. 1, pressure was raised to 13 MPa twice. Subsequently, the artificial flaw was added on the tank, and then in each of the water pressure proof tests Nos. 2 and 3, pressure was raised to 13 MPa once. Finally, in the water pressure proof test No. 4, pressure was raised until the tank was ruptured.

4. Damage of tank after test

4.1 Confirmation of Kaiser effect

The Kaiser effect refers to a phenomenon in which when a test object is sound after removing a preload and then placing

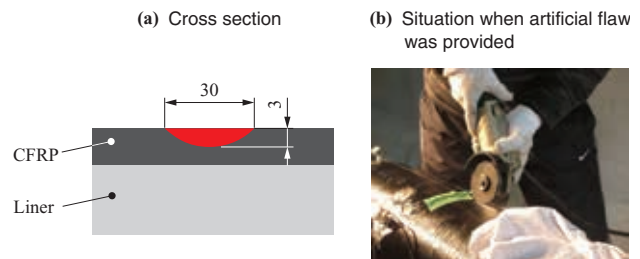


Fig. 3 Damage point (unit : mm)

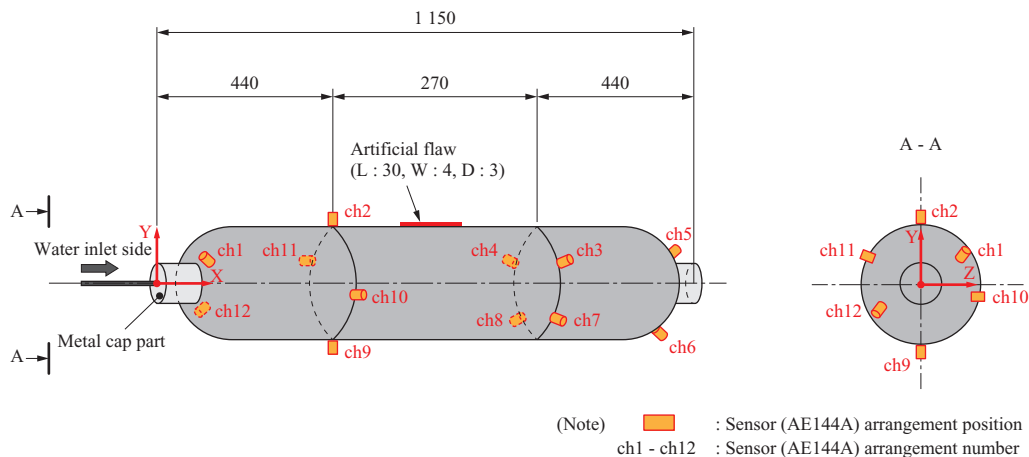
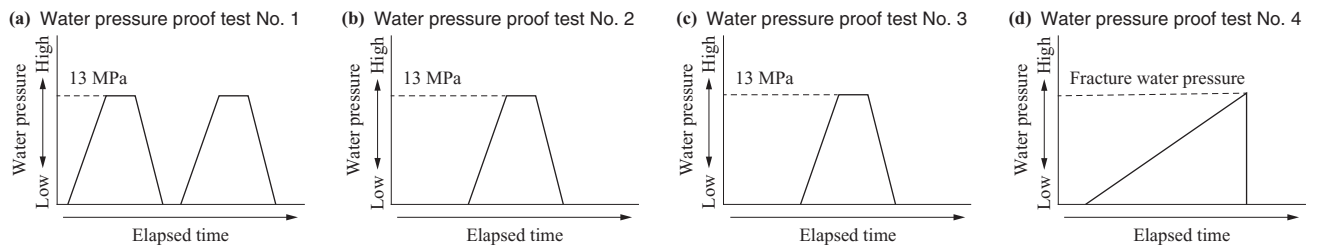


Fig. 2 Sensor location and damage point (unit : mm)



(Note) (b), (c) and (d) illustrate the steps of the water pressure proof test after providing the artificial flaw.

Fig. 4 Underwater propagation test

a load again, AE is hardly detected at up to the preload condition. Since this does not appear in a structurally unstable stage like a stage where destruction is in progress, it can be utilized for the test as an index of structural stability⁽⁸⁾.

Figure 5 illustrates the numbers of AE hits per second in the water pressure proof tests Nos. 1 and 2. In **Fig. 5**, the green line represents water pressure. Also, the horizontal axis represents an elapsed time from the start of the test, the left vertical axis the number of hits, and the right vertical axis the water pressure. From **Fig. 5**, it was confirmed that in the water pressure proof test No. 1, the pressure was raised to 13 MPa twice, and in the second pressure raising process, no hit was found at up to 13 MPa, in other words, the Kaiser effect held. Note that the reason why AE hits were found at around 13 MPa (around 360 s) in the second pressure raising process was that the pressure was unstable and exceeded 13 MPa. In the water pressure proof test No. 2 after providing the artificial flaw, it was confirmed that hits were measured at 8 MPa or larger, and the Kaiser effect did not hold. This may be because in the pressure raising process to 13 MPa, a new crack occurred and the damage of the tank developed.

4.2 Change of damaged point

Figure 6 illustrates the change of the damaged point between after providing the artificial flaw (-**(a)**) and after the water pressure proof test No. 2 (-**(b)**). From **Fig. 6**, it was confirmed that after the water pressure proof test No. 2, a crack occurred on the bottom surface of the artificial flaw point. It was also confirmed that the crack propagated from the edge of the artificial flaw point in the circumferential direction of the tank.

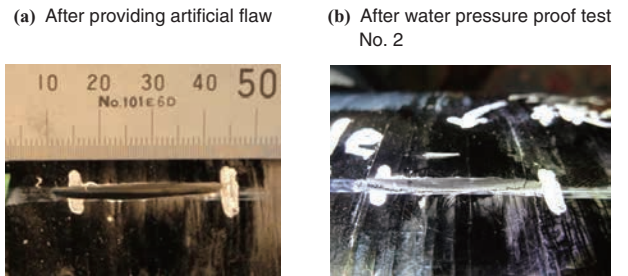


Fig. 6 Change of damaged point

5. Three-dimensional source location using underwater propagation waves

5.1 Separation between surface propagation waves and underwater propagation waves

For the three-dimensional source location described in this report, it is necessary to use only data on AE propagating under water. However, in AE data measured in this test, surface propagation waves and underwater propagation waves were mixed. Setting measurement conditions does not make it easy to measure only the underwater propagation waves, and the settings must be changed every time a measurement target is changed. For this reason, when performing the source location analysis after the measurement, both were separated. **Figure 7** illustrates area locating.

The separation was attempted by, in consideration of angles formed between sound sources and the reception sensors, determining reception sensors used for the analysis on a certain region.

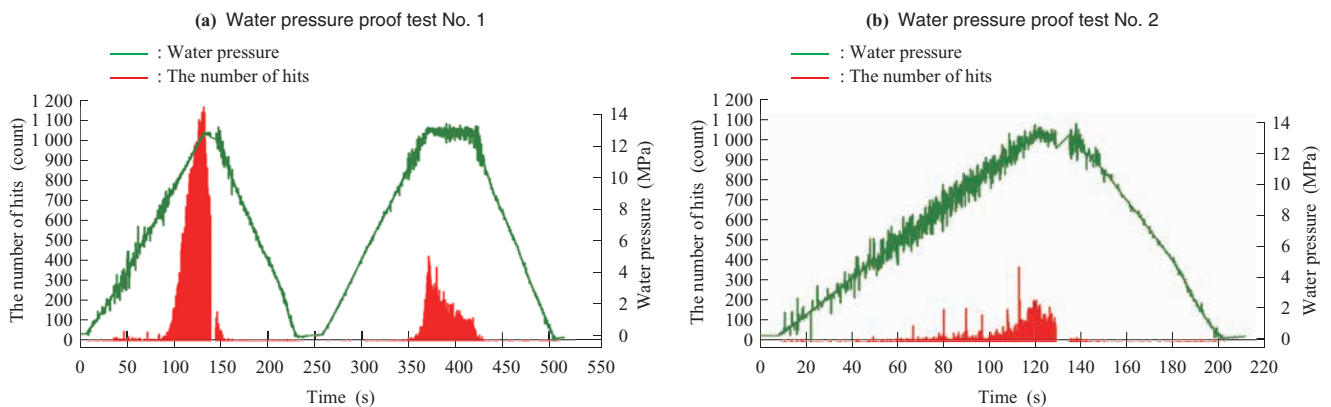


Fig. 5 AE hits per second

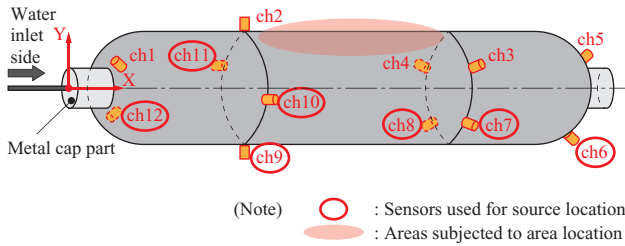


Fig. 7 Area location

5.2 Directivity of underwater propagation wave

In order to determine reception sensors used for the analysis, it is necessary to take account of the directivity of the underwater propagation waves. Using VS150-RIC (oscillator diameter : $\phi 20$ mm) as an emission source and AE144A (oscillator diameter : $\phi 10$ mm) as a reception sensor, the relationship between the angle formed by the emission source and the reception sensor and relative echo height was calculated as a theoretical value. A reason to use VS150-RIC with $\phi 20$ mm as the emission source is that VS150-RIC is larger in oscillation diameter than AE144, resulting in high directivity, and therefore easily obtain the directivity of the underwater propagation waves. Figure 8 illustrates the theoretical value and measured value of the relative echo height with respect to the angle between the emission source and the reception sensor. From Fig. 8, it turns out that the measured value and the theoretical value both are close in value at up to 90° , and in particular, at up to 60° , have very close values. From this result, we thought that within the range where the angle between the AE emission source and the reception sensor is 0 to 60° , the underwater propagation waves can be obtained.

5.3 Area location

An area for the source location was determined using Visual AE software (by Vallen, Germany). Figure 9 illustrates a polygon processor. As viewed from the front Fig. 9-(a), the vessel was divided into three areas, whereas as viewed from the water inlet side -(b), it was divided into two areas. By

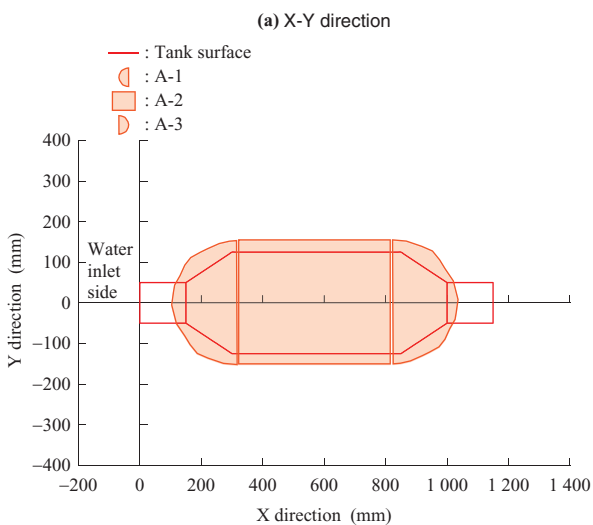


Fig. 9 Polygon processor

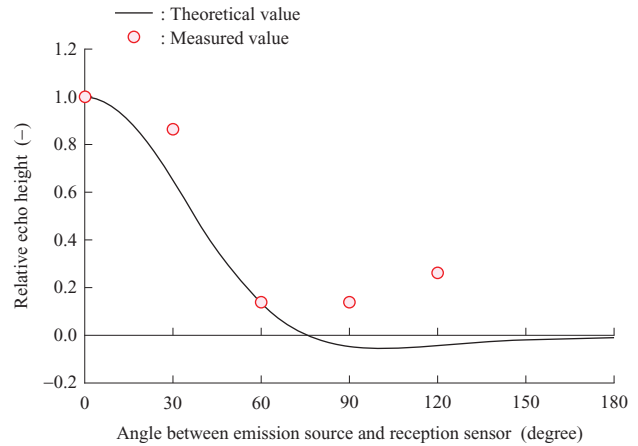


Fig. 8 Angle of source/receiving sensor and echo height

combining any two of the divided areas, a total of six areas (① A-1 and B-1, ② A-2 and C-1, ③ A-3 and B-1, ④ A-1 and B-2, ⑤ A-2 and C-2, and ⑥ A-3 and B-2) were defined. Figure 10 illustrates the six divided areas. This sort of source location method was referred to as area location.

5.4 Results of three-dimensional source location using underwater propagation waves

Each of the six areas described in the previous section was subjected to the source location by designated sensors. For example, the red area at the top of the tank illustrated in Fig. 7 corresponds to the area ③, which was subjected to the source location by the ch6 to ch12 sensors.

Figures 11 and 12 illustrates the results of the three-

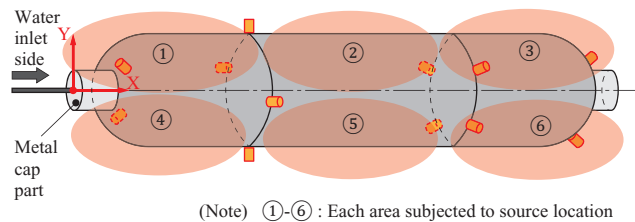


Fig. 10 Six divisions

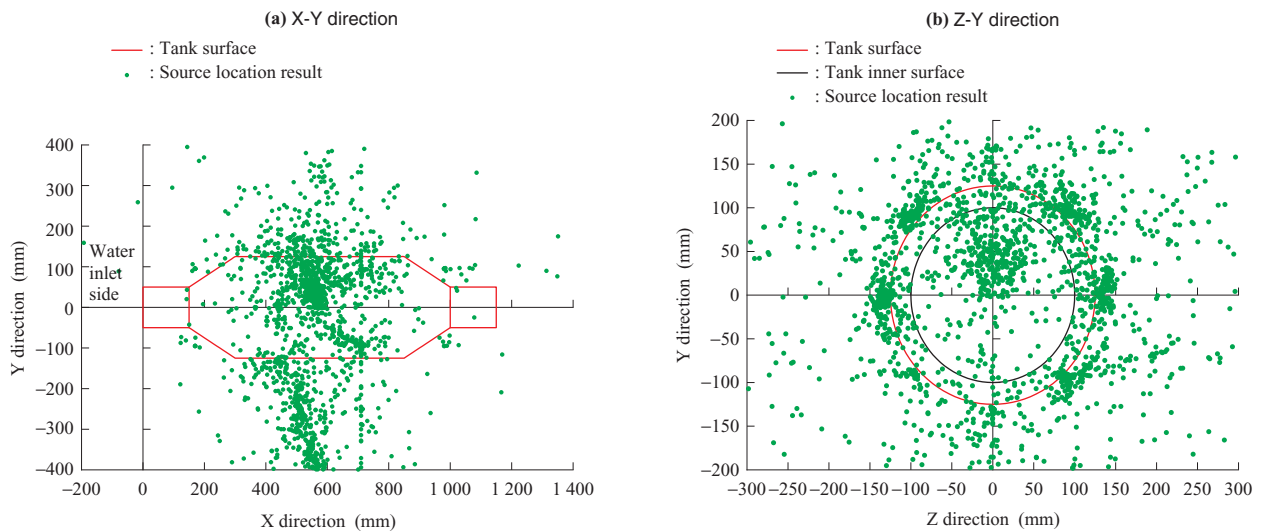


Fig. 11 3D source location using all AE data

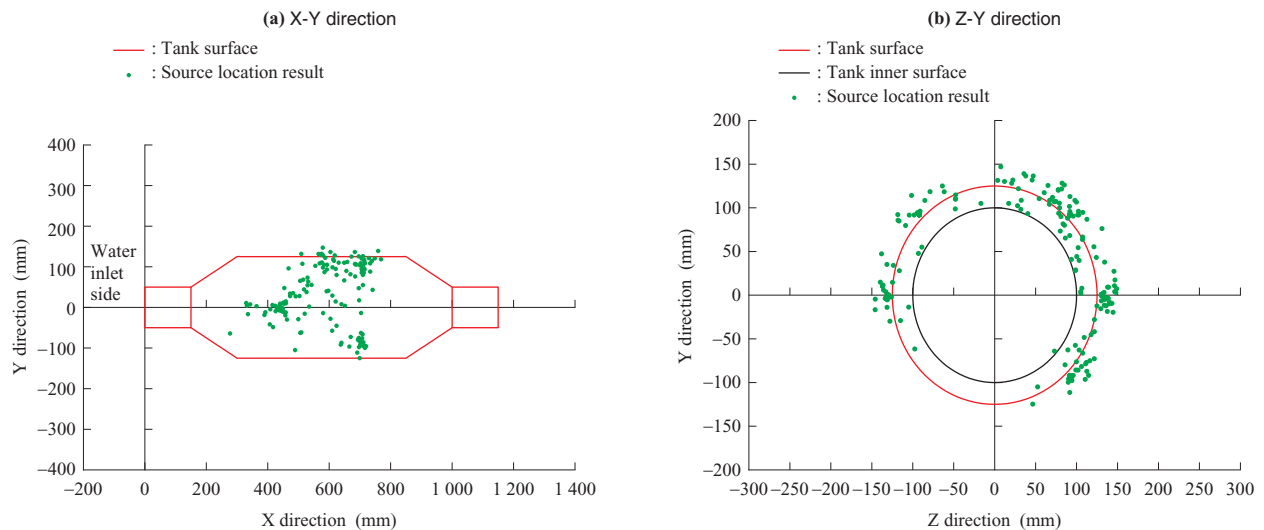


Fig. 12 3D source location using "Area locating"

dimensional source location based on all pieces of data and the results of the three-dimensional source location based on the area location. **Figure 11** illustrates the results obtained using the all pieces of measurement data without any area division, and **Fig. 12** illustrates the results based on the area location. **Figures 11-(a)** and **12-(a)** are plan views with the X direction as the horizontal axis, the Y direction as the vertical axis, and the water inlet side set on the left side. Also, **Figs. 11-(b)** and **12-(b)** are plan views as viewed from the water inlet side with the Z direction as the horizontal axis and the Y direction as the vertical axis. Green dots in these diagrams represent the source location results, and the positions of the dots represent AE emission sources.

From **Fig. 11**, it turns out that the location results are concentrated in the upper part of the tank. However, many results lie outside the tank and under water where no AE is supposed to occur. On the other hand, from **Fig. 12**, it turns out that the location results are not present both inside and

outside the tank, and concentrated in the upper part of the tank.

From the above three-dimensional source location results using the underwater propagation waves, we obtained the following findings.

- (1) In the water pressure proof test, the three-dimensional source location can be performed using the AE signals propagating under water.
- (2) The area location enabled the surface propagation waves and the underwater propagation waves to be well separated, and consequently the location results were concentrated in the upper part of the tank near the damaged point.

6. Conclusion

In the water pressure proof test of the CFRP tank having a carbon fiber winding thickness of 6 mm, the three-dimensional source location based on AE that occurred when damage was

developed by raising pressure and propagated under water was performed. As a result, the three-dimensional source location only using the AE signals propagating under water (area location) showed that the location results were concentrated in the upper part of the tank near the damaged point. Although this report still remains within qualitative evaluation, we will grasp the fracture mechanism of the CFRP material and examine the size of damage applicable with the source location in the future.

REFERENCES

- (1) ASME Boiler and Pressure Vessel Code, Section V Article 12 : Acoustic Emission Examination of Metallic Vessels during Pressure testing American Society for Mechanical Engineers Latest edition
- (2) ASME Boiler and Pressure Vessel Code, Section V Article 11 : Acoustic Emission Examination of Fiber Reinforced Plastic Vessels American Society for Mechanical Engineers Latest edition
- (3) High Pressure Institute of Japan : HPI TR G 110: 2017, Recommended Practice for Acoustic Emission Evaluation of Corrosion Damage in Bottom Plate of Oil Storage Tanks (in Japanese) High Pressure Institute of Japan (2017)
- (4) A. Kaneko and M. Takemoto : AE Propagation Behavior in a Liquid-Loading Cylindrical Tank (in Japanese) Journal of JSNDI Vol. 51 No. 11 (2002) pp. 718-725
- (5) S. Murakami, K. Homma, T. Koike and M. Yamada : AE Source Location Using Neural Network on AE Evaluation of Floor Conditions in Above-Ground Tank Journal of Solid Mechanics and Materials Engineering Vol. 1 No. 7 (2007. 3) pp. 919-930
- (6) H. Nakamura, T. Arakawa, K. Sekine, N. Kasai, M. Maeda and H. Suzuki : Examination of Identification and Removal Method for Drop Noise at AE Measurement of a Tank (in Japanese) Journal of High Pressure Institute of Japan Vol. 46 No. 1 (2008) pp. 26-31
- (7) T. Nakajima, H. Kawasaki and A. Sato : Experimental Consideration about AE Sources Location of a Thin CFRP Vessel Pressure Test (in Japanese) Transactions of the Japan Society of Mechanical Engineers Series A Vol. 79 No. 797 (2013) pp. 115-118
- (8) The Japanese Society for Non-Destructive Inspection : Acoustic Emission Testing II (in Japanese) (2008) p. 8